2D Fluid Model for Axisymmetric RF Ion Thruster Cylindrical Discharge Chamber

Emre Turkoz* and Murat Celik†

Bogazici University, Istanbul, 34342, Turkey

Radio-Frequency (RF) ion thrusters are impulse generators to be used at in-space applications. Inductively coupled plasma (ICP) is generated by using electromagnetic heating through the utilization of a number of axisymmetric coils in the discharge chamber of an RF ion thruster. A numerical model is built to investigate the underlying physics of the ICP in RF ion thrusters. The model solves the Maxwell's equations through magnetic vector potential equation and assumes that the ICP can be assumed to obey the continuum approach. Approximations are applied to the equations of motion for electrons, ions and neutrals to facilitate the simulations. Finite volume method for compressible gases is adapted for the ICP and results show the same tendency as previous models and experiments.

Nomenclature

A	Magnetic vector potential
E	Electric field
B	Magnetic field
n	Number density
v	Velocity field
ν	Collision frequency
Q	Energy flux
$\bar{R}$	Particle generation
ϕ	Plasma potential
Γ	Particle flux
k	Boltzmann's constant
ω	Radio-frequency
P	Power

Subscript

i	Ion species
n	Neutral species
e	Electron species

I. Introduction

THE radio-frequency (RF) ion engine, which is also known as RF ion thruster, is an impulse generator for small thrust values. Examples from the literature[1] indicate that the thrust of a typical ion engine is varying from 10 mN to 200 mN with specific impulse values ranging from 2500 to 5500 sec. It is a plasma-based device which utilizes electrostatic force between grids to accelerate ionized gas out of the discharge chamber to generate thrust. The representation of a typical RF ion engine is given in figure 1. The plasma in RF ion thruster discharge chamber is an inductively coupled plasma (ICP). In order to understand the underlying physics, for further optimization and in the course of digital prototyping, building a numerical

---

*Graduate Student, Mechanical Engineering, Bogazici University.
†Assistant Professor, Mechanical Engineering, Bogazici University.

American Institute of Aeronautics and Astronautics

model for the ICP in the discharge chamber is of great importance. RF ion thruster modeling is a recently developing area and a complete model is yet to be developed. This work aims to build a numerical model for the ICP in RF ion thrusters.

A recent numerical study on RF ion thrusters can be seen in Tsay's work.[3] The model presented in that work approximates the plasma as a fluid continuum, and solves the continuity and momentum equations for electron and ion velocities and particle densities in 2D axisymmetric domain. The model fails to track neutrals, since it assumes that the neutrals are stationary. The neutral conservation equation is solved on global scale along with the electron temperature equation, which again fails to provide spatial values for these properties. And due to the fact that it requires a correction coefficient for its equations, which is derived for each thruster configuration after some tests, it fails to provide a model which can be used for digital prototyping.

Stein[4] gives an example of PIC/DSMC algorithms used for kinetic modeling of the plasma in the discharge chamber. Mistoco[5] performed one of the most recent works on the RF ion thruster modeling. This work focuses on miniature scale thrusters and lays down a 1D kinetic model for ICP of the discharge chamber. But the inductively coupling between coil and plasma is not described. Goebel[6] develops a 0D model which yields very good accordance with practical applications but lacks to give the spatial distribution of plasma parameters.

Figure 1. Geometry of an RF ion thruster discharge chamber[2]

The RF ion thruster relies on ICP physics. Therefore advances in ICP modeling are directly related to RF ion thruster modeling. Lieberman[7] offers a numerical model for inductively coupled plasma. Even though the application area of the cited paper is for plasma etching operations, the model presented is valid for any inductively coupled plasma charge configuration. Suekane[8] presented a simpler version of inductively coupled plasma model for plasma torches, which we took benefit of while developing our model. Hammond[9] built a 2D fluid model of the inductively coupled plasma, which is an example for treating the electron energy equation. Hsu[10] also provided numerical models for inductively coupled plasma, incorporating energy equations for electrons and also other species along with the boundary conditions.

Even though extensive work is performed on ICP, the lack of a complete model of RF ion thruster configuration is apparent. With this work, we aim to close this gap by applying the right boundary conditions and formulating other terms according to the configuration physics. Within the scope of this work, a complete model is developed for the three species: ions, neutrals and electrons which are assumed to obey the continuum approach in this particular application. The implementation of this model is performed within the in-house developed plasma physics simulations platform named AETHER. For this particular application many approximations are applied to eliminate some of the equations from the full model.

This paper is organized as follows: In section II, the description of the problem solved in this study is presented. In the key section of this paper, section III, the two components, electromagnetic model and the fluid model, of the numerical model are elaborated. The approximations for the fluid model are presented and the final form of the equations to be solved are listed. Within this section boundary conditions are also given. In section IV, the numerical method to solve this problem is elaborated and the algorithm is given. In section V, the results of the model are presented. The concluding remarks are given in section VI.

II. Problem Statement

The problem consists of evaluating the plasma parameters of a cylindrical discharge chamber. The chamber is assumed to have the same dimensions as the RIT15-LP thruster. It has 15 cm diameter and 7 cm chamber length. 13 coils are assumed to be wrapped around the chamber with a constant RF current magnitude of 6 A. The RF frequency is 2 MHz.

The solution domain is represented in figure 2. The figure presents the domain with a representative structured mesh employed in the solution. The inlet is assumed to be 4 cm in diameter and the neutral influx is taken as 2 sccm. The outlet grid is assumed to have a 0.5 ion optical transparency and the neutral transparency is assumed to be 0.5.
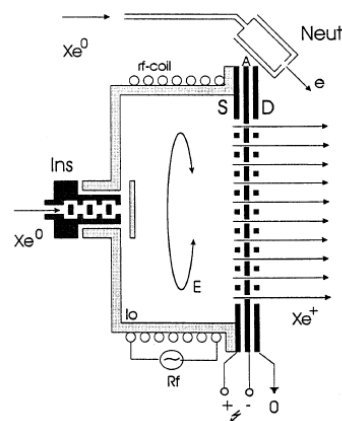
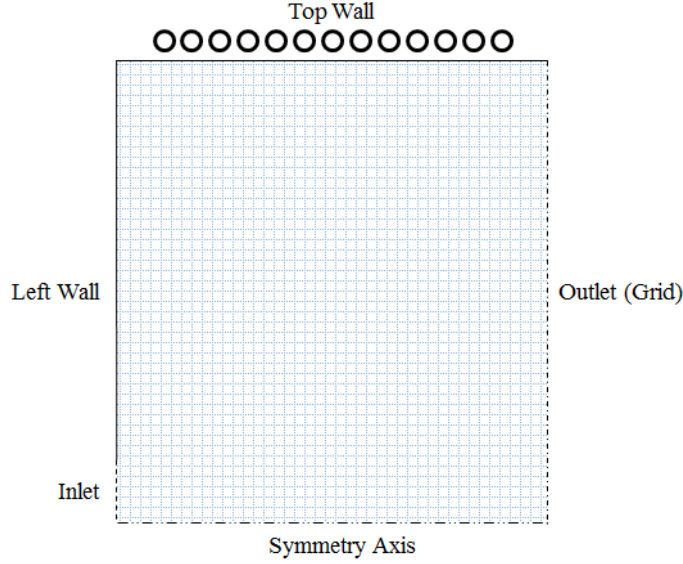American Institute of Aeronautics and Astronautics

Figure 2. Representation of the solution domain - the discharge chamber of RIT15-LP

III. Numerical model

The model presented in this work consists of two main components and it is formulated for 2D axisymmetric domains in cylindrical coordinates. Electromagnetic model handles the coil and ICP coupling through magnetic vector potential, whereas the fluid model solves for the plasma parameters using fluid continuum approximation. The electric and magnetic fields evaluated from the electromagnetic model is applied to the momentum equations in the fluid model as Lorentz force. Furthermore the azimuthal electric field heats up the electrons and deposits energy into the plasma. The other way of coupling is applied through the calculation of the plasma conductivity. Plasma conductivity is calculated with the parameters evaluated in the fluid model and applied to the electromagnetic model to evaluate the electromagnetic fields for the next time step.

A. Electromagnetic Model

In the beginning of the solution procedure, electromagnetic model solves the magnetic vector potential equation. This equation is formulated[8] as:

$$\nabla^2 \mathbf{A} = \mu_0 \sigma \frac{\partial \mathbf{A}}{\partial t} \tag{1}$$

where $\mathbf{A}$ is defined as the magnetic vector potential and formulated as $\nabla \times \mathbf{A} = \mathbf{B}$, where $\mathbf{B}$ is the magnetic field.

The electric field is obtained by taking the time derivative of the magnetic vector potential, which is in the azimuthal direction. Additionally, there is also an additional contribution the electric field from the plasma potential gradient. This plasma potential is calculated by imposing the quasi-neutrality condition through divergence-free current formulation which will be elaborated in the next section.

The electric field is also calculated from:

$$\mathbf{E} = -\nabla \phi - \frac{\partial \mathbf{A}}{\partial t} \tag{2}$$

B. Fluid Model

The calculated electric and magnetic fields are incorporated into the fluid equations. Fluid equations consist of continuity and momentum equations for the three species. In addition, electron energy balance equation is solved to calculate the electron temperature distribution. These equations can be listed as below:

American Institute of Aeronautics and Astronautics

Continuity equations:

$$\frac{\partial n_i}{\partial t} + \nabla \cdot (n_i \mathbf{v_i}) = \dot{R}_i \tag{3}$$

$$\frac{\partial n_e}{\partial t} + \nabla \cdot (n_e \mathbf{v_e}) = \dot{R}_e \tag{4}$$

$$\frac{\partial n_n}{\partial t} + \nabla \cdot (n_n \mathbf{v_n}) = -\dot{R}_i \tag{5}$$

Momentum equations:

$$m_i n_i \left(\frac{\partial \mathbf{v_i}}{\partial t} + \mathbf{v_i} \cdot \nabla \mathbf{v_i} \right) + k \nabla (n_i T_i) = e n_i \mathbf{E} + e n_i \mathbf{v_i} \times \mathbf{B} - m_i n_i \nu_{in} (\mathbf{v_i} - \mathbf{v_n}) - m_i n_i \nu_{ei} (\mathbf{v_i} - \mathbf{v_e}) \tag{6}$$

$$m_e n_e \left(\frac{\partial \mathbf{v_e}}{\partial t} + \mathbf{v_e} \cdot \nabla \mathbf{v_e} \right) + k \nabla (n_e T_e) = -e n_e \mathbf{E} - e n_e \mathbf{v_e} \times \mathbf{B} - m_e n_e \nu_{en} (\mathbf{v_e} - \mathbf{v_n}) - m_e n_e \nu_{ei} (\mathbf{v_e} - \mathbf{v_i}) \tag{7}$$

$$m_n n_n \left(\frac{\partial \mathbf{v_n}}{\partial t} + \mathbf{v_n} \cdot \nabla \mathbf{v_n} \right) + k \nabla (n_n T_n) = -m_n n_n \nu_{in} (\mathbf{v_n} - \mathbf{v_i}) - m_n n_n \nu_{en} (\mathbf{v_n} - \mathbf{v_e}) \tag{8}$$

The energy balance for electrons:

$$\frac{3}{2} \frac{\partial}{\partial t} (n_e e T_e) + \nabla \cdot \mathbf{Q_e} = -e \mathbf{E_a} \cdot \mathbf{\Gamma_e} + P_{dep} - P_{coll} \tag{9}$$

So, the fluid model consists of the solutions for the 7 equations given above for the 7 parameters: n_i, n_e, n_n, $\mathbf{v_i}$, $\mathbf{v_e}$, $\mathbf{v_n}$ and T_e. These parameters represent ion number density, electron number density, neutral number density, ion velocity, electron velocity, neutral velocity and electron temperature, respectively.

The terms $\dot{R}_i$, $\dot{R}_e$, and $\dot{R}_n$ denote the ion, electron and neutral density generation terms. The terms ν_{in}, ν_{ei} and ν_{en} denote ion-neutral, electron-ion and electron-neutral collision frequencies, respectively. k is Boltzmann's constant, e is elementary electron charge. T_i, T_n, and T_e are ion, neutral and electron temperatures, respectively. P_{dep} denotes the power deposited to the plasma, P_{coll} denotes the power loss due to collisions. $\mathbf{\Gamma_e}$ is the electron flux, and $\mathbf{Q_e}$ is the electron energy flux. $\mathbf{E_a}$ is the ambipolar electric field.

Momentum equations in the model consist of three components for each species. Axial, radial and azimuthal velocity components for each species are calculated. With these nine equations coming from momentum equtions, along with the two equations coming from the real and complex parts of the magnetic vector potential equation, three continuity equations and one energy equation, the model is closed with a total of 15 equations.

1. Approximations and Final Form of Model Equations

The code is developed to solve all of the equations presented in the previous section, but the particular application allows to make approximations to reduce nonlinearities and therefore fasten the simulation. The most important approximation is the drift-diffusion approximation for the electrons. According to this approximation:

- The inertia terms for the electrons are negligible.

- Ion and neutral velocities are very low compared to the electron velocity. Therefore we can neglect those terms also.

With these approximations, the equation of motion for electrons becomes:

$$m_e n_e (\nu_{ei} + \nu_{en}) \mathbf{v_e} = -\nabla P_e - e n_e \mathbf{E} - e n_e v_{e,\theta} \times \mathbf{B} \tag{10}$$

We call $\nu_{eff} = \nu_{ei} + \nu_{en}$ and the pressure gradient for the ideal gas assumption is formulated as: $\nabla P_e = k \nabla (n_e T_e)$. Inserting these expressions and dividing both sides with $m_e \nu_{eff}$:

$$\mathbf{\Gamma}_e = n_e \mathbf{v}_e = -\frac{k T_e}{m_e \nu_{eff}} \nabla n_e - \frac{e n_e}{m_e \nu_{eff}} (\mathbf{E} + v_{e,\theta} \times \mathbf{B}) \tag{11}$$

This part of the discussion is really important since it considers the driving mechanism for maintaining the quasi-neutrality: the plasma potential. The potential induced in the plasma builds up an electric field in r-z plane that regulates the motion of the ions and electrons so that they can be kept in accordance to maintain the quasi-neutrality. Inserting the proper expression for the electric field given in (2), the electron particle flux becomes:

$$\Gamma_e = n_e \mathbf{v}_e = -\frac{kT_e}{m_e \nu_{eff}} \nabla n_e - \frac{k n_e}{m_e \nu_{eff}} \nabla T_e + \frac{e n_e}{m_e \nu_{eff}} \left(\nabla \phi + \frac{\partial \mathbf{A}}{\partial t} - v_{e,\theta} \times \mathbf{B} \right) \tag{12}$$

It is worth to notice that the magnetic vector potential is nonzero only in the azimuthal direction. Therefore the electric field resulting from this potential affects only the azimuthal velocity. Even though this formulation simplifies the equations for the electrons by eliminating the nonlinear terms, it does not eliminate the variables and also introduces one extra variable called electric potential. This requires the introduction of an another equation to solve for this parameter. Here we introduce the divergence-free current constraint:

$$\nabla \cdot \mathbf{j} = \nabla \cdot (n_i \mathbf{v}_i - n_e \mathbf{v}_e) = 0 \tag{13}$$

This formulation imposes the quasi-neutrality by equating $n_e = n_i$. This equation is obtained by subtracting the ion continuity equation from the electron continuity equation.

Plugging the electron particle flux evaluated above from the drift-diffusion approximation into the divergence-free current formulation yields the equation for electric potential in r-z plane:

$$\nabla \cdot \left(n_i \mathbf{v}_i + \frac{kT_e}{m_e \nu_{eff}} \nabla n_e + \frac{k n_e}{m_e \nu_{eff}} \nabla T_e - \frac{e n_e}{m_e \nu_{eff}} \nabla \phi + \frac{e n_e}{m_e \nu_{eff}} (v_{e,\theta} \times \mathbf{B}) \right) = 0 \tag{14}$$

Multiplying the whole expression with the elementary charge e to obtain expressions containing the plasma conductivity and moving the electric potential term to the other side of the equation:

$$\nabla \cdot (\sigma \nabla \phi) = e \nabla \cdot (n_i \mathbf{v}_i) + \nabla \cdot \left(\frac{ekT_e}{m_e \nu_{eff}} \nabla n_e \right) + \nabla \cdot \left(\frac{ek n_e}{m_e \nu_{eff}} \nabla T_e \right) + \nabla \cdot (\sigma (v_{e,\theta} \times \mathbf{B})) \tag{15}$$

where the plasma conductivity is defined as:

$$\sigma = \frac{n_e e^2}{m_e \nu_{eff}} \tag{16}$$

This formulation is necessary to satisfy the quasi-neutrality in this particular application. With this formulation the model equations solved can be listed as follows:

- Magnetic vector potential (1)

- Axial, radial and azimuthal ion and neutral velocities using the full form as given in equations (6) and (8)

- Electron flux in axial and radial direction using drift-diffusuion approximation (12)

- Electron temperature (9)

- Plasma potential (15)

C. Boundary Conditions

The solution domain, the structured mesh, is assumed to extend up to the presheath region, which indicates the beginning of the sheath region. The sheath region itself is not resolved since it would be computationally very expensive to reduce the mesh size to the Debye length. Sheath region is not solved in the model, therefore presheath boundary conditions[3] are imposed on the walls.

To evaluate the boundary conditions, two different regions are considered as shown in figure 3. The solution domain extends up to the boundary between plasma and the sheath. Since there is no particle generation in the sheath region, the particle flux leaving the plasma is equal to the particle plasma reaching the wall at steady state.
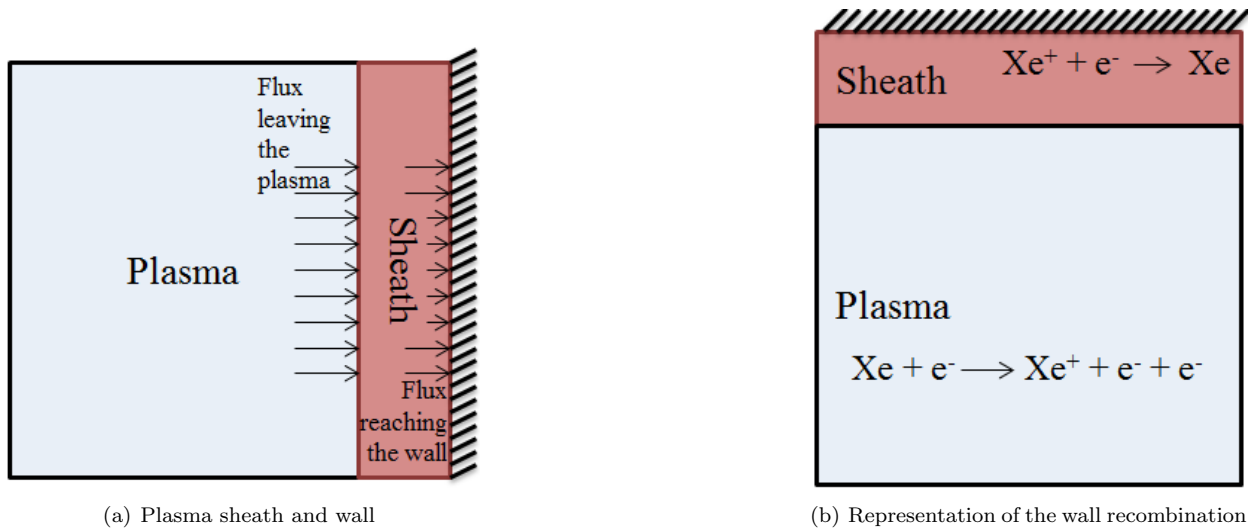
American Institute of Aeronautics and Astronautics

(a) Plasma sheath and wall

(b) Representation of the wall recombination

Figure 3. Axial velocities for ions and neutrals

Ions that leave the plasma and reach the wall are assumed to go back into the system with wall recombination as neutrals. This wall recombination contributes to the formulation of the boundary condition of the neutrals. The wall recombination is presented in figure 3.

In an inductively coupled plasma, the quasi-neutrality condition is imposed, which denotes the equal amount of positive and negative charges in the plasma. This condition is satisfied by the ambipolar diffusion, where a balancing electric field occurs between charged particles so that the fluxes leaving the plasma are the same. This requires the condition to equate the ion and electron fluxes to the wall. This yields:

$$\Gamma_{i,wall} = \Gamma_{e,wall} \tag{17}$$

$$n_i u_B = \frac{n_e \bar{v}_e}{4} exp\left(-\frac{e\Delta\phi}{kT}\right) \tag{18}$$

where u_B denotes the Bohm velocity defined as:

$$u_B = \sqrt{\frac{kT_e}{m_i}} \tag{19}$$

To impose the equality of ion and electron flux, instead of evaluating the velocity for the electrons, we can impose the following condition:

$$n_i u_B = n_e v_e \tag{20}$$

$$v_e = \frac{n_i u_B}{n_e} \tag{21}$$

This formulation yields electron velocity in boundary nodes. Since imposing either velocity or a pressure condition is enough for a self-consistent solution, after we impose the formulation above for the electron velocity and the Bohm velocity for the ions, the pressure, in this case the number density, is evaluated with the numerical method implemented. The remaining species in this case is the neutrals.

The neutrals have the thermal velocity in random directions. But since the neutral velocity does not get affected in any way from the sheath, the directional thermal velocities are cancelled by the term in the reverse directions so that the thermal velocity does not have a directional contribution. Therefore the only remaining term is due to the wall recombination:

$$\Gamma_{n,wall} = -\gamma\Gamma_{i,wall} \tag{22}$$

where γ denotes the ratio of the ions recombine at the wall, which in our study is taken to be equal to 1. Then the neutral velocity is defined as:

$$v_n = -\gamma\frac{n_i u_B}{n_n} \tag{23}$$

As it is the case with electrons and ions, the number density of the neutrals are evaluated using the numerical method.

In RF thruster applications an electrostatic field is generated between electrically conductive grids. These grids are called screen and accelerator grids. They let some particles out and prevent a portion of them to stay in the discharge chamber. They have an optical transparency for ions and an overall grid transparency for neutrals.

In this study we denote the optical ion transparency with ϕ_i and the overall grid transparency with ϕ_n. Therefore the flux boundary conditions on the outlet grid is denoted as:

$$\Gamma_{n,outlet} = -\gamma \Gamma_{i,wall}(1 - \phi_i) + \phi_n n_n u_n \tag{24}$$

The relation above indicates that the portion of the ions that can not get through the grids hits the grid and returns as neutrals to the system. The second term in the relation is the application of the grid transparency on the neutral motion. The neutral velocity to be used in this expression assuming that the normal flux to the grid wall is conserved for neutrals.

IV.   Solution Technique

The two models described above are solved on cylindrical coordinate system with structured grids. The magnetic vector potential equation within the electromagnetic model is discretized with second order finite differencing scheme. This equation is solved fully explicit in time. On the other hand, fluid equations are solved fully implicit in time to ensure convergence and numerical stability. For the fluid equations, the finite volume method is used. The finite volume method utilizes cells generated with the mesh and equations are discretized by evaluating the flux balance in each of these control volumes. The discretization of the equations are performed within the SIMPLE algorithm framework as described in literature.[11] Plasma is represented as a compressible flow and the discretization is performed accordingly relying on the examples.[12]
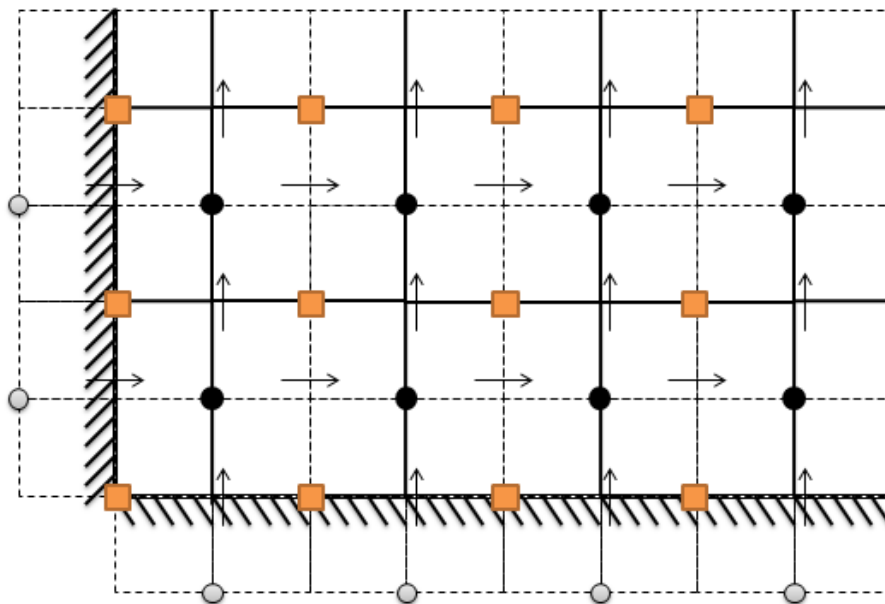

Figure 4. Staggered grid used in solving the problem. Vertical arrows denote the radial velocity, horizontal arrows denote the axial velocity. Rectangles denote the electromagnetic fields and circles denote the number densities and temperature

The structured grid is 51×51. The coefficient matrices in the fluid model is solved with ILU-preconditioned GMRES method that is implemented within the in-house coding package developed for this study. The equations are solved successively and self consistently at each time step through inner iterations. After the equations converge, the solution marches in time and starts to solve for the variables in the next time step.

American Institute of Aeronautics and Astronautics

V. Results

The RF frequency for this particular problem is 2 MHz as stated in section II. The frequency indicates that a full cycle of the alternating current takes 5.0E-7 seconds. The time step for the electromagnetic model is determined as 6E-11 seconds and for the fluid model the time step is 1.2E-08 seconds. The code reaches steady state after 25 cycles. The problem is solved with in-house developed AETHER plasma simulations code on a 2-processor Xeon (E5-2643) workstation. The code marches 2 cycles per hour.

The steady state is reached when the total number of particles approach a constant value. As stated above, the model solves for the ions and neutrals. Hence, the number of neutrals and ions should converge to a constant value. The contour plots below shows the solutions when the code reaches the steady state.

The electron temperature turns out to vary in each cycle harmonically as expected. It reaches a mean value of 3.61 eV as can be seen in figure 5. The cycle ratio in this figure denotes the time passed in terms of RF cycles.
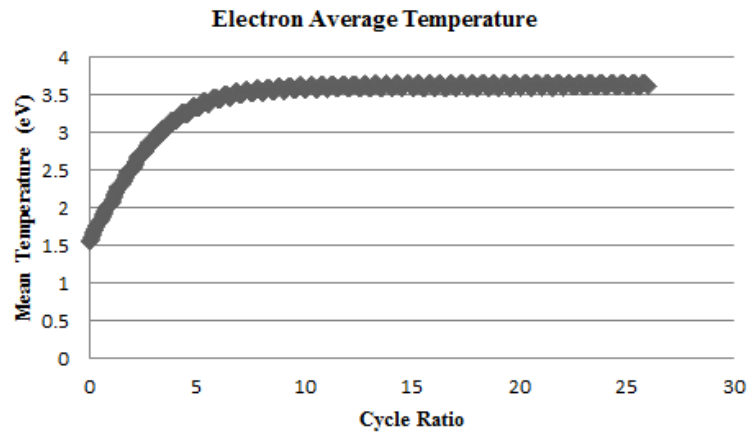

Figure 5. Electron average temperature after 25 cycles

The axial particle velocities are evaluated as expected. As it can be seen from figure 6, ions rush out from the plasma with Bohm velocity at the presheath boundary. The ion outflux corresponds to neutral influx as the ions recombine at the wall and turn back into the system as neutrals. The location of the inlet flux of 2 sccm is apparent in the figure.
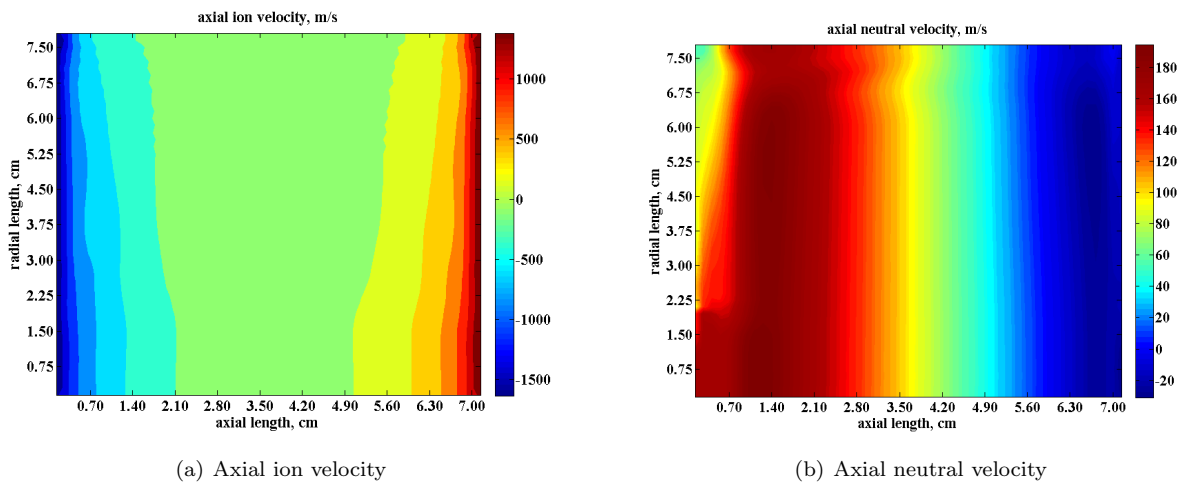

(a) Axial ion velocity

(b) Axial neutral velocity

Figure 6. Axial velocities for ions and neutrals

The electron temperature distribution is shown in the figure 7. The distribution shows that the electrons

American Institute of Aeronautics and Astronautics

are colder towards the bottom left corner of the domain which is expected because neutrals are fed into the system in this region. Also the maximum electron temperature is observed in the region where the power deposition is also at its peak values. In the same figure the spatial plasma density distribution is presented. Plasma distribution obtained in this figure shows the same tendency observed in examples from the literature.[3, 13]

(a) Electron temperature distribution
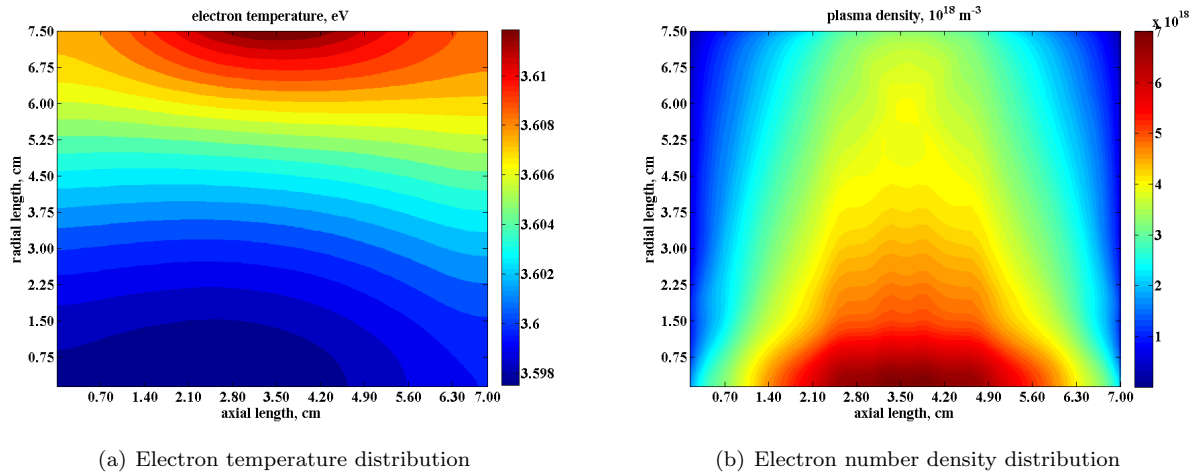

(b) Electron number density distribution

Figure 7. Electron temperature and number density distributions

The power deposition in a cycle changes as the current fluctuates with time in a sinusoidal manner as shown in figure 8. It is observed that the power deposition reaches peak values at 0.25 and 0.75 cycles but with a small penetration into the plasma. The largest power deposition penetration into the plasma occurs at 0.375 and 0.875 cycle ratios. The peak value for power deposition in the figure below is 0.2 W.
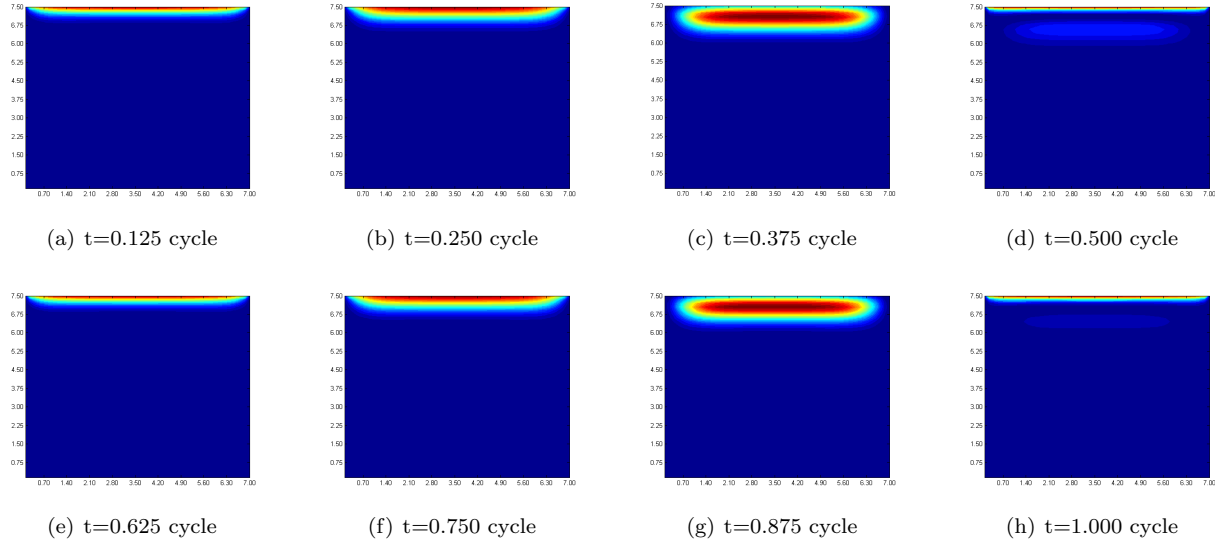

(a) t=0.125 cycle

(b) t=0.250 cycle

(c) t=0.375 cycle

(d) t=0.500 cycle

(e) t=0.625 cycle

(f) t=0.750 cycle

(g) t=0.875 cycle

(h) t=1.000 cycle

Figure 8. Power deposition

VI.   Conclusion

A self consistent ICP model for RF ion thrusters is successfully developed and implemented. The proposed model solves for the number densities and velocity components in 3D for ions and neutrals. Electron properties are evaluated using the drift-diffusion approximation and spatial electron temperature distribution is also calculated. The results are consistent with the examples from the literature. The power deposition

American Institute of Aeronautics and Astronautics

and the plasma density distribution have the same contour map as depicted in previous works on RF ion thruster discharge simulations.[3,13] The implementation of the 0D model by Goebel[6] also yields a mean temperature of 3.31 eV for RIT15-LP ion thruster, which is very close to the temperature values evaluated in this work.

Neglecting the convective terms and the time dependence from the electron equation of motion facilitates the simulation to a great degree. If the convective terms for the electron species are desired to be implemented, the required time step should be much lower than the current one used in the simulation for ions and neutrals, which are much heavier species. Furthermore, the mesh required for this application is required to be much finer, on the order of the Debye length, to cover the electron velocity.

The ion transparency in this work is assumed to be known beforehand. But it is to our knowledge that the ion transparency should be evaluated by including the ion optics physics. Examples of this type of work include ffx[14] or CEX2D, CEX3D.[15] As the future work, an ion optics code can be incorporated into the scheme devleoped in this work.

In practice, the RF ion thrusters are set into application through a matching circuit to ensure maximum power deposition. It is very common to simulate this matching network through modeling the network and the plasma as two sides of an air-core transformer.[3,16] This transformer model determines the amount of current to be supplied at each instant for maximum power deposition taking plasma resistance and inductance into account. The implementation of a transformer model is left as future work.

References

[1]Leiter, H., Killinger, R., Bassner, H., Kukies, R., and Mueller, J., "Evaluation of the Performance of the Advanced 200mN Radio-Frequency Ion Thruster RIT-XT," 38th *Joint Propulsion Conference and Exhibit*, Indianapolis, IN, July 2002, AIAA–2002–3836.

[2]Leiter, H. J., Killinger, R., Bassner, H., Muller, J., Kukies, R., and Frohlich, T., "Development and performance of the advanced radio frequency ion thruster RIT-XT," 28th *International Electric Propulsion Conference (IEPC 2003)*, 2003.

[3]Tsay, M., "Two-Dimensional Numerical Modeling of Radio-Frequency Ion Engine Discharge," Ph.D. Thesis, Massachusetts Institute of Technology, Cambridge, USA, 2011.

[4]Stein, W. B., Alexeenko, A. A., and Hrbud, I., "Performance Modeling of an RF Coaxial Plasma Thruster," 43rd *Joint Propulsion Conference and Exhibit*, Cincinnati, OH, July 2007, AIAA 2007-5292.

[5]Mistoco, V. F., "Modeling of Small Scale Radio-Frequency Inductive Discharges for Electric Propulsion Applications,," PhD. Thesis, The Pennsylvania State University, University Park, PA, 2011.

[6]Goebel, D., "Analytical Discharge Model for RF Ion Thrusters," *Plasma Science, IEEE Transactions on*, Vol. 36, No. 5, October 2008, pp. 2111 –2121.

[7]Kawamura, E., Graves, D. B., and Lieberman, M. A., "Fast 2D hybrid fluid-analytical simulation of inductive/capacitive discharges," *Plasma Sources Science and Technology*, Vol. 20, No. 3, 2011, pp. 035009.

[8]Suekane, T., Taya, T., Okuno, Y., and Kabashima, S., "Numerical studies on the nonequilibrium inductively coupled plasma with metal vapor ionization," *Plasma Science, IEEE Transactions on*, Vol. 24, No. 3, June 1996, pp. 1147 –1154.

[9]Hammond, E., Mahesh, K., and Moin, P., "A Numerical Method to Simulate Radio-Frequency Plasma Discharges," *Journal of Computational Physics*, Vol. 176, No. 2, 2002, pp. 402 – 429.

[10]Hsu, C.-C., Nierode, M. A., Coburn, J. W., and Graves, D. B., "Comparison of model and experiment for Ar, Ar/O 2 and Ar/O 2 /Cl 2 inductively coupled plasmas," *Journal of Physics D: Applied Physics*, Vol. 39, No. 15, 2006, pp. 3272.

[11]Versteeg, H. and Malalasekera, W., *An Introduction to Computational Fluid Dynamics - The Finite Volume Method*, Prenctice Hall, Essex, England, 1995.

[12]Ferziger, J. H. and Peric, M., *Computational Methods for Fluid Dynamics, 3rd Edition*, Springer-Verlag, Berlin, 2002.

[13]Takao, Y., Eriguchi, K., and Ono, K., "Two-Dimensional Particle-in-Cell Simulation of a Micro RF Ion Thruster," 32nd *International Electric Propulsion Conference*, Wiesbaden, Germany, September 2011, IEPC-2011-076.

[14]Farnell, C. C., Williams, J. D., and Wilbur, P. J., *Numerical Simulation of Ion Thruster Optics*, National Aeronautics and Space Administration, Glenn Research Center, 2003.

[15]Anderson, J. R., Katz, I., and Goebel, D., *Numerical simulation of two-grid ion optics using a 3D code*, Pasadena, CA: Jet Propulsion Laboratory, National Aeronautics and Space Administration, 2004.

[16]Piejak, R., Godyak, V., and Alexandrovich, B., "A simple analysis of an inductive RF discharge," *Plasma Sources Science and Technology*, Vol. 1, No. 3, 1992, pp. 179.